Iranian Journal of Science & Technology, Transaction B, Engineering, Vol. 33, No. B5, pp 415-424
Printed in The Islamic Republic of Iran, 2009

INCEPTION OF TRANSFORMATION OF HEMATITE TO MAGNETITE DURING MECHANICAL ACTIVATION: A THERMODYNAMICAL APPROACH*

M. SAHEBARY, S. RAYGAN**, S. A. SEYED EBRAHIMI AND H. ABDIZADEH

School of Metallurgy and Materials Engineering, Faculity of Engineering, University of Tehran, Tehran, I. R. of Iran, Email: shraygan@ut.ac.ir

Abstract– In this research the thermodynamic of mechanochemical activation by high energy milling of hematite has been studied. It has been shown that transformation reaction due to ball milling of α-Fe_2O_3 has been started after 15 hours milling. As the sum of amorphization and dislocation energies is a suitable approximation of total stored energy, the contribution of these two energies has been identified. The contribution of amorphization and dislocation energies after 15 hours milling have been calculated at about 76 and 9 kJ/mol, respectively. Thus, the increase in molar enthalpy of milled hematite is about 85 kJ/mol. The total Gibbs free energy of mechanochemical transformation of hematite to magnetite after 15 hours milling has also been determined. The temperature for transformation of activated hematite to magnetite has been calculated at about 300 K. The bulk temperature of powder after 15 hours milling has been measured at about 325 K. Therefore, at this temperature hematite cannot be stable and will transform to magnetite during milling.

Keywords– Hematite, magnetite, stored energy, mechanical activation

1. INTRODUCTION

The iron oxides; hematite, maghemite and magnetite; are important electrical and magnetic materials. These oxides are conventionally prepared by oxidation–reduction process at elevated temperatures. Mechanochemical treatment is an alternating process to produce fine particles of these oxides.

During the last two decades, extensive studies have been made on the transformation reactions induced due to ball milling of hematite in various milling conditions. Kaczmarek and Ninham [1, 2] produced magnetite from hematite through ball milling in various milling atmospheres, i.e. vacuum, argon and air. The reverse transformation, magnetite to hematite, was explained to occur by ball milling in air [3]. Zdujic *et al*. [4, 5] explained the transformation process of α-Fe_2O_3 to Fe_3O_4 and subsequently to FeO. They stated that transferring of sufficient energy to the particles was necessary to change the thermodynamical stability of α-Fe_2O_3 to Fe_3O_4 and subsequently to FeO. Randrianantoandro *et al*. [6] showed that the α-Fe_2O_3 to γ-Fe_2O_3 phase transformation could be induced by mechanical grinding within an ethanol medium. They showed that during high energy milling process, the oxide powders were exposed essentially to the compressive and shearing stresses. Mitov *et al*. [7] investigated the mechanochemical activation of magnetite and maghemite with close structures and different cation distributions. They demonstrated that the different rates of phase transformations could be explained by a phonon mechanism of energy dissipation for maghemite and a mixed phonon-electron mechanism for magnetite. Novikov [8], by means of X-ray diffraction and Mössbauer spectroscopy, demonstrated that the discrepancies in the available data on the cation distribution in cation-deficient compounds could be

*Received by the editors January 8, 2008; Accepted June 22, 2009.
**Corresponding author

associated with the structural features of $Fe_{3-v}O_4$ compounds. Hofmann, Campbell and Kaczmarek [9-14] made comprehensive studies on the production of deficient magnetite from hematite by ball milling. Their comparisons by means of neutron diffraction patterns of as-milled samples at room temperature and 950 K combined with chemical analysis indicated that a significant fraction of the milled products had a disordered or amorphous form. They calculated the maximum fraction of γ-Fe_2O_3 at about 8%. The formation of γ-Fe_2O_3 was likely to be due to a shearing transformation involving movement of the oxygen included planes. They also concluded that the main transformation of α-Fe_2O_3 to $Fe_{3-v}O_4$ occurred by rupturing of the surface layers of α-Fe_2O_3. This rupture led to a release of oxygen and transformation of α-Fe_2O_3 to $Fe_{3-v}O_4$.

Although the mechanism of transformation of hematite to magnetite has been studied by various researchers, they have not showed the onset conditions of transformation and the way of thermodynamic functions changes. The present study attempts to gain a deeper insight into the thermodynamical features of this solid state reduction. In other words, the aim of this study is to clarify, for the first time, the reason of transformation of activated hematite to magnetite during ball milling at room temperature from a thermodynamic point of view.

2. EXPERIMENTAL PROCEDURE

Commercial grade α-Fe_2O_3 powder of 99% purity with particle size of 30-60 microns was used as the starting material. Mechanochemical treatment was performed in a planetary ball mill, Fritsch Pulverized 6. A hardened steel vial of 250 cm^3 volume filled with hardened steel balls of 20 mm diameter was used for milling. In all experiments, the ball to powder mass ratio was 25:1 with a powder mass of 20 g. All milling experiments were performed in 300 rpm under air atmosphere without any additives. It should be pointed out that the milling experiments were carried out under closed milling conditions, i.e. the vial was not opened during all the milling periods. Different milling times 2, 5, 10, 15, 20, 30, 45, 60, 75 and 90 h were considered in order to follow the solid state reactions. The morphology of the milled particles was studied by scanning electron microscopy (PHILIPS XL30) and their crystallographic structure was investigated by Philips PW-1730 X-ray diffractometer (XRD) using Cu Kα radiation.

3. RESULTS AND DISCUSSION

Figure 1 shows The XRD patterns of milled powder in various milling times. The patterns of the starting powder and the powders milled up to 10 hours show only the presence of α-Fe_2O_3 phase. It is seen that after 2 hours milling the peaks intensity decrease significantly due to the decrease of the size of hematite crystallites. The traces of magnetite can be observed after 15 hours milling. Although Fe_3O_4, is crystallographically isomorphous with γ-Fe_2O_3, having a lattice parameter ($a \approx 0.840$ nm) slightly larger than that of γ-Fe_2O_3 ($a \approx 0.835$ nm) [15], but according to the Hofmann *et al*. [9, 11] studies it can be concluded that a large amount of powder should be magnetite.

a) Energy contributions

Heegn [16] has reported that the following structural defects illustrate the energetic condition of mechanically activated solids:

(1) Dislocation concentration with its specific energy;
(2) Degree of amorphization with its energy;
(3) Surface area to the surroundings or to a second phase with its specific energy;

Pourghahramani [17, 18] has proved that the contribution of amorphization energy to the total energy changes is about 93–98.5%. Similar energy distributions are found for quartz, calcite, magnesite, kaolinite,

iron and periclase [17]. It is concluded that the sum of amorphization and dislocation energy is a suitable approximation of total energy.

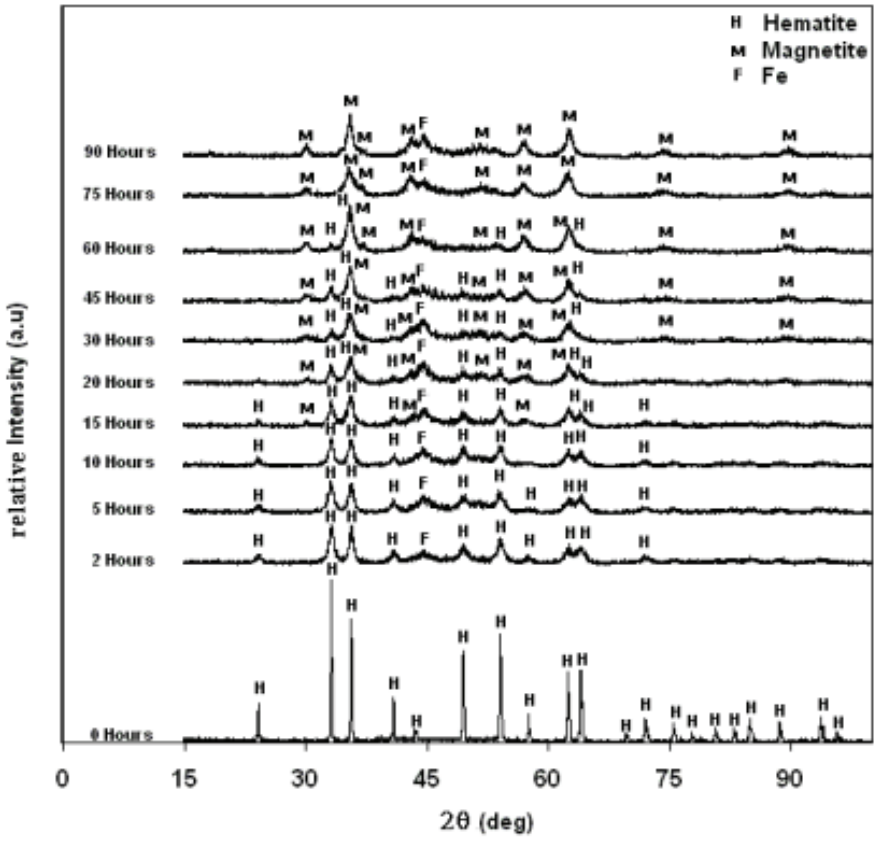

Fig. 1. XRD patterns of α -Fe_2O_3 powder milled for various milling times.

1. Energy contribution of dislocations: The classical energy balance studies on the propagation of a small crack in an elastically isotropic solid establish a functional relationship between the critical tensile stress for crack propagation and flaw size [19]. Other studies propose that such ideal behavior does not apply to the majority of crack sensitive materials and should be modified [19]. Such modifications can be applied where crack tip plasticity is confined to a small plastic enclave in an elastic matrix, leading to a recast of Griffith's ideas in terms of fracture mechanics concepts:

$$K_{1C} = Y\sigma_C (a)^{1/2} \tag{1}$$

where K_{1C} is the critical stress intensity factor for crack propagation, Y is a geometrical factor related to the shape of the crack, σ_c is critical tensile stress for crack propagation and (a) is the flaw size. This equation shows that by decreasing flaw size, (a), higher tensile stresses are needed to propagate a crack, i.e. $\sigma_c \sim (a)^{-1/2}$. Hence, initial fracture and size reduction of hematite occurs by propagation of the largest flaws at relatively low σ_c. With increasing stored energy by milling, the particle and its flaw size decrease to micron or submicron in which σ_c becomes very large. This stored energy generates more dislocations rather than fracture of particles [20]. Figure 2 shows the SEM micrograph of 10 hours milled α-Fe_2O_3 in comparison with the initial powder. The effect of ball milling on the morphology and size distribution of powders has been previously investigated by Moshksar [21]. In this research, clusters of particles are formed during milling but decreasing the size of particles in Fig. 2b is in good agreement with the above discussions.

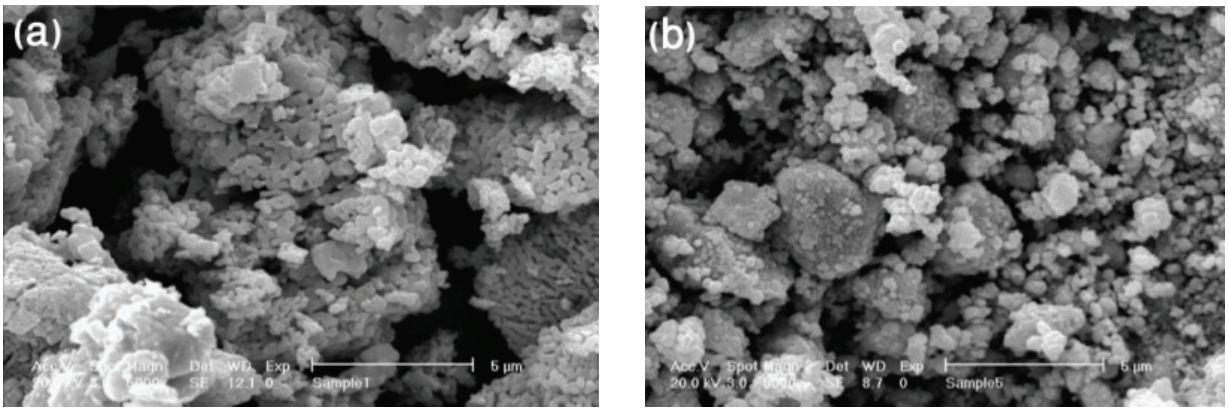

Fig. 2. SEM micrograph of hematite particle. a) before milling, b) after 10 hours milling.

The increase in molar Gibbs free energy of milled hematite due to dislocations, ΔG_d, is related to the changes in molar enthalpy ΔH_d and molar entropy ΔS_d associated with these dislocations:

$$\Delta G_d = \Delta H_d - T\Delta S_d \tag{2}$$

According to Cottrell hypothesis, the dislocations entropy is small. Thus, compared to ΔH_d, $T\Delta S_d$ is negligible [22]. Hence, ΔG_d is almost equal to:

$$\Delta G_d \approx \Delta H_d = \rho_d m_V \left(\frac{b^2 \mu_s}{4\pi}\right) \ln\left(\frac{2\rho_d^{-1/2}}{b}\right) \tag{3}$$

where b is Burger's vector of the dislocation, μ_s is the elastic shear modulus, ρ_d is the dislocation density and m_V is the molar volume of hematite [20]. This equation provides a quantitative estimation of the increase in molar free energy (stored energy) due to dislocations.

The direction of Burger's vector of hematite is similar to Corundum [17]. Therefore, the length of Burger's vector of hematite can be estimated as 5.03×10^{-10} m [17]. $M_V = 3.047\times10^{-5}$ m^3mol^{-1} is the molecular weight of hematite (0.15969 kg mol^{-1}) divided by its density 5240 (kg m^{-3}) [23]. The value of μ_s which is equal to 225 GPa, represents an average value for hematite polycrystalline aggregates [24]. The minimal dislocation density of polycrystalline hematite powders has been calculated using the following formula [2, 17, 25]

$$\rho_d = \frac{3}{d^2} \tag{4}$$

where d is average crystallite size (m). Williamson–Hall approach can be used to estimate the crystallite size of the ball milled hematite powders [26]. The calculated mean crystallite size from XRD patterns which is corrected for instrumental broadening has been drawn versus milling time of Fe_2O_3 in Fig. 3.

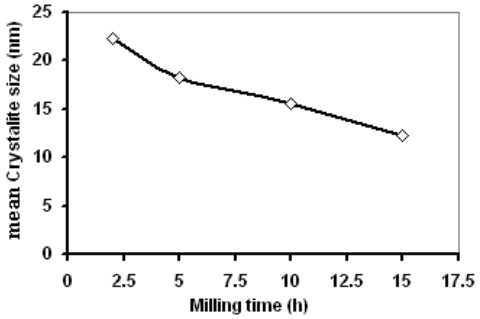

Fig. 3. Mean crystallite size against milling time for α -Fe_2O_3.

The calculated dislocation density according to equation 4 up to 15 hours milling is shown in Fig. 4. The effect of dislocation density on the stored energy of hematite powders is shown in Fig. 5. It is obvious that the stored energy (ΔH_d) increases with increasing the milling time.

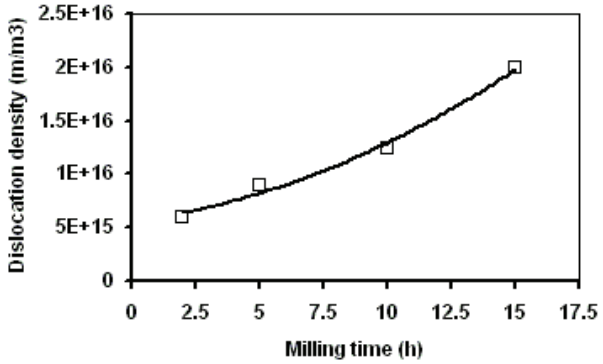

Fig. 4. Dislocation density of α-Fe_2O_3 powder milled for various milling times.

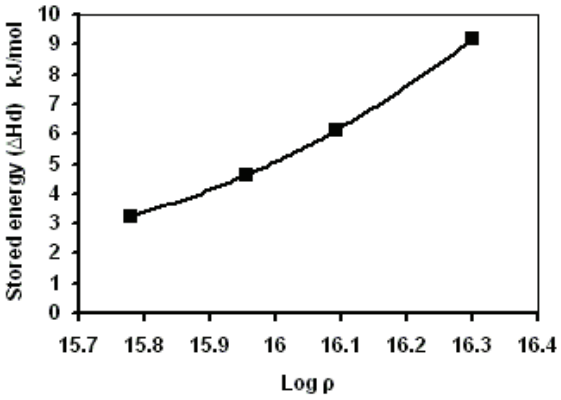

Fig. 5. Effect of dislocation density on stored energy, ΔH_d, of hematite powder.

2. Energy contribution of amorphization: The content of the amorphous phase has been determined by the equation proposed by Ohlberg and Stickler [27]. The degree of crystallinity is defined as:

$$X = \frac{U_o}{I_o}\frac{I_X}{U_X}100 \tag{5}$$

where U_o and U_x refer to the background intensity of non-activated and activated hematite, respectively. I_o and I_X are also integral intensities of diffraction lines of non-activated and activated hematite.

In order to estimate the amount of amorphous phase after each milling time, the average relative intensity $\left(\frac{I_X}{I_o} \text{ and } \frac{U_X}{U_o}\right)$ of the four intensive peaks of milled hematite, (2θ=24, 33, 41, 49.5 degrees) has been calculated. The change of the intensities of the above mentioned peaks of the hematite after 15 hours milling has been given in Fig. 6.

Then, amorphization energy of milled hematite could be estimated as:

$$\Delta H_{am} = \left[1 - \left(\frac{U_o}{I_o}\frac{I_X}{U_X}\right)\right]\Delta\overline{H}_{am} \tag{6}$$

where $\Delta\overline{H}_{am} = 90.99$ (kJ.mol^{-1}) is molar amorphization energy of hematite [28]. The energy contributions of dislocation density, ΔH_d, amorphization, ΔH_{am}, and overall change in enthalpy, $\sum\Delta H$, are shown in Fig. 7.

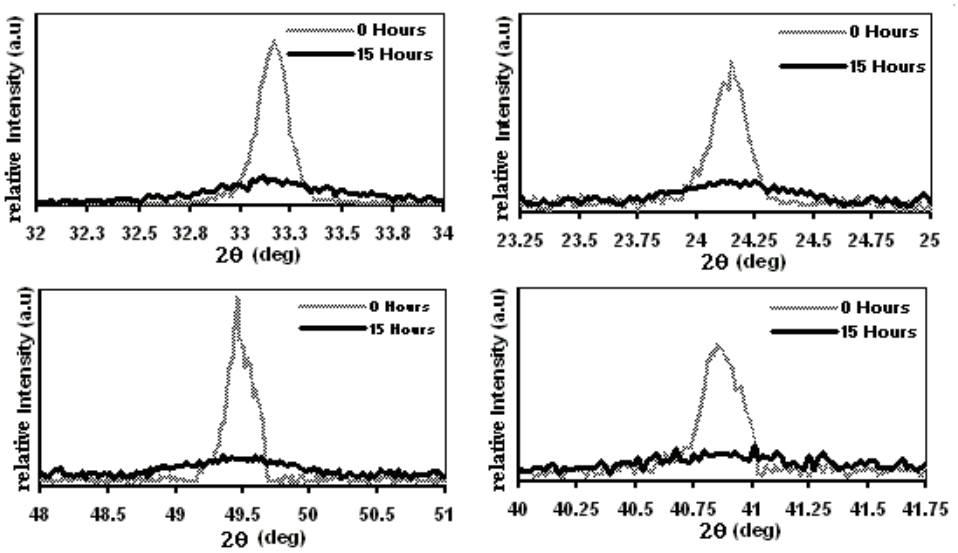

Fig. 6. Amorphization of 15 hours milled powder compared to initial powder.

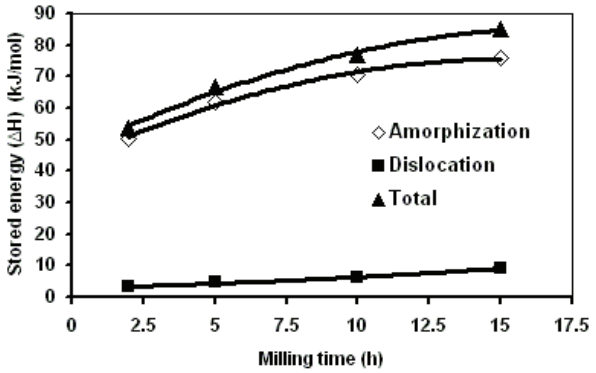

Fig. 7. Energy contributions of dislocation, amorphization, in total stored energy.

It is obvious that transferring sufficient energy to the hematite particles is necessary to start the transformation of hematite to magnetite. Figure 7 shows that the contribution of amorphization and dislocation energy up to 15 hours milling (starting of magnetite formation) are 76 and 9 kJ.mol^{-1}, respectively. Therefore, the increase in molar total enthalpy (required molar stored energy for transformation) of milled hematite prior to transformation to magnetite should be about 85 kJ/mol.

b) Estimation of molar Gibbs free energy of milled hematite

The following reaction has been considered to estimate the molar Gibbs free energy of milled hematite:

$$Fe_2O_3 = 2/3Fe_3O_4 + 1/6O_2 \qquad (7)$$

where the standard Gibbs free energy of this reaction is [4]:

$$\Delta G^o = G_2^o - G_1^o = 116596.67 - 67.8T \qquad \text{J.mol}^{-1} \qquad (8)$$

and at the ambient pressure:

$$\Delta G = \Delta G° + RT\ln P_{O_2}^{1/6} = 116596.67 - 67.8T + 8.314T\ln(0.2)^{1/6} = 116596.67 - 70.03T \text{ J.mol}^{-1} \quad (9)$$

According to this equation, the equilibrium temperature is 1665 K. Therefore, magnetite cannot be stable below 1665 K.

During high energy ball milling up to 15 hours, the energy level of hematite, G^{o}_{1}, will increase to $G_1^0 + \Delta G_d + \left[1 - \left(\frac{U_o}{I_o}\frac{I_X}{U_X}\right)\right](\Delta \overline{G}_{am})_T$ and ΔG becomes:

$$\Delta G = G_2^0 - (G_1^0 + \Delta G_d + \left[1 - \left(\frac{U_o}{I_o}\frac{I_X}{U_X}\right)\right].(\Delta \overline{G}_{am})_T) + RT\ln P_{O_2}^{1/6} \quad (10)$$

$$\Delta G = \Delta G° + RT\ln P_{O_2}^{1/6} - \Delta G_d - \left[1 - \left(\frac{U_o}{I_o}\frac{I_X}{U_X}\right)\right].(\Delta \overline{G}_{am})_T \quad (11)$$

while ΔG_d and $\left[1 - \left(\frac{U_o}{I_o}\frac{I_X}{U_X}\right)\right](\Delta \overline{G}_{am})_T$ are the increase in molar Gibbs free energy of milled particles due to dislocation and amorphization, respectively. ΔG_d has been calculated before in Eq. (3). Due to the similarity of the amorphous phase and liquid phase, ΔG_{am} could also be calculated by the following equation [20]:

$$(\Delta G_{am})_T = \left(\frac{H_F}{T_m}\right)(T_m - T) \quad (12)$$

where H_F is the enthalpy of fusion at the melting point (T_m) and $(\Delta G_{am})_T$ is the estimated change in molar Gibbs free energy due to amorphization. By substituting 122.9 kJ.mol^{-1} and 1895 K as the enthalpy of fusion and melting point of hematite, ΔG_{am} becomes [29]:

$$(\Delta G_{am})_T = 122900 - 64.85T \text{ J.mol}^{-1} \quad (13)$$

According to equation (11), the total change in molar Gibbs free energy of milled hematite could be estimated as:

$$\Delta G = 116596.67 - 67.8T + RT\ln P_{O_2}^{1/6} - \rho_d M_V \left(b^2 \mu_S / 4\pi\right) \ln\left(2\rho_d^{-1/2} / b\right) - \left[1 - \left(\frac{U_o}{I_o}\frac{I_X}{U_X}\right)\right](122900 - 64.85T) \quad (14)$$

and finally:

$$\Delta G = 4765.67 - 15.89T \text{ J.mol}^{-1} \quad (15)$$

Figure 8 shows the ΔG of non-activated and activated hematite versus temperature according to Eqs. (9) and (15). According to this figure, the equilibrium temperature for the 15 hours milled powder is 300K, above which the α-Fe_2O_3 phase is not stable and the reaction proceeds toward the formation of Fe_3O_4.

The vial temperature (bulk temperature of the powder) after 15 hours milling has been measured by thermometer at about 325 K. It can be seen from Fig. 8 that at this temperature, ΔG of reaction (7) in the activated condition is negative. Therefore it proceeds toward the formation of magnetite.

It should be mentioned that the calculation of ΔG according to equation 15 at temperatures above 600 K is meaningless and excluded from Fig. 8 because high temperature can recover the disorder structure by recrystallization of the amorphous phase and decrease dislocation density. The negative value of ΔG near 325 K shows that formation of magnetite has been started a few moments before the 15 hours milling.

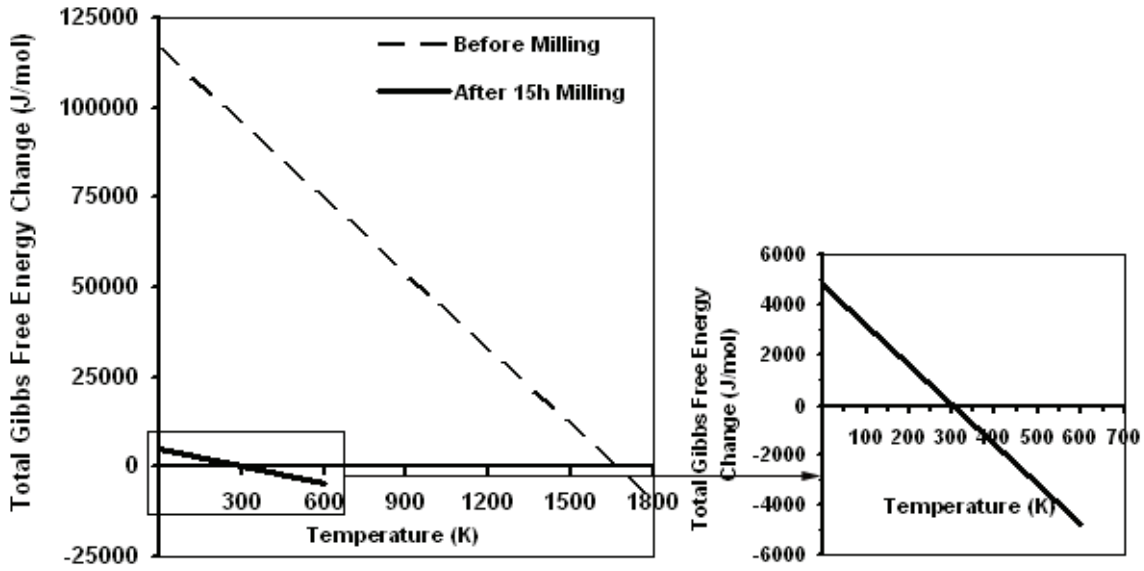

Fig. 8. Total Gibbs free energy of mechanochemical reaction before and after 15hours milling

4. CONCLUSION

The results of this investigation suggest that:

1) The increase in molar enthalpy (required molar stored energy for transformation) of milled hematite prior to transformation to magnetite is about 85 $kJ.mol^{-1}$.
2) The contribution of amorphization and dislocation energy in total stored energy up to 15 hours milling (starting of magnetite formation) is 76 and 9 $kJ.mol^{-1}$ respectively.
3) According to the calculated total Gibbs free energy function of mechanochemical reaction after 15 hours milling the transformation temperature is about 300 K.
4) At the bulk temperature of the powder, the total Gibbs free energy function of 15 hours milled powder is negative and reaction proceeds toward the formation of magnetite.
5) The negative value of ΔG near 325 K shows that formation of magnetite has started a few moments before the 15 hours milling.

REFERENCES

1. Kaczmarek, W. A. & Ninham, B. W. (1994). Preparation of Fe_30_4 and γ-Fe_2O_3 powders by magnetomechanical activation of hematite. *IEEE Trans. Magn*., Vol. 30, pp. 732–734.
2. Kaczmarek, W. A., Onyszkiewicz, I., Ninham, B. W. (1994). Structural and magnetic characteristic of novel method of $Fe_20_3 \rightarrow Fe_30_4$ reduction by magnetomechanical activation. *IEEE Trans. Magn*., Vol. 30, pp. 4725–4727.
3. Linderoth, S. L., Jiang, J. Z. & Morup, S. (1997). Reversible α-Fe_2O_3 to Fe_3O_4 transformation during ball milling. *Mater. Sci. Forum*, pp. 235–238, pp. 205–210.

4. Zdujic, M., Jovalekic, C., Karanovic, L. J., Mitric, M., Poleti, D. & Skala, D. (1998). Mechanochemical treatment of α-Fe_2O_3 powder in air atmosphere. *Mater. Sci. Eng*., A245, pp. 109–117.
5. Zdujic, M., Jovalekic, C., Karanovic, L. J. & Mitric, M. (1999). The ball milling induced transformation of α-Fe_2O_3 powder in air and oxygen atmosphere. *Mater Sci Eng.*, Vol. A262, pp. 204–213.
6. Randrianantoandro, N., Mercier, A. M., Hervieu, M., & Greneche, J. M. (2001). Direct phase transformation from hematite to maghemite during high energy ball milling. Mater. Lett., Vol. 47, pp. 150–158.
7. Mitov, I., Cherkezova-Zheleva, Z., Mitrov, V. (1997). Comparative study of the mechanochemical activation of magnetite (Fe_3O_4) and maghemite (γ-Fe_2O_3). *Phys. Status Solidi (a)*, Vol. 161, pp. 475–482.
8. Novikov, S. I., Lebedeva, E. M., Schtoltz, A. K., Yurchenko, L. I., Tsurin, V. A. & Barinov, V. A. (2002). Distribution of cations in magnetite prepared by mechanochemical synthesis. *Phys. Solid State*, Vol. 44, pp. 124–132.
9. Hofmann, M., Campbell, S. J., Kaczmarek, W. A., Welzel, S. & Alloys, J. (2003). Mechanochemical transformation of α-Fe_2O_3 to $Fe_{3-x}O_4$ –microstructural investigation. *Compd*., Vol. 348, pp. 278–284.
10. Campbell, S. J., Kaczmarek, W. A., Wang, G. M. (1995). Mechanochemical transformation of haematite to magnetite. *NanoStruct. Mater*., Vol. 6, pp. 735–738.
11. Campbell, S. J., Klingelhofer, G., Kaczmarek, W. A., Hofmann, M., Nagel, R. & Wang, G. (2002). Mechanochemical transformations in α-Fe_2O_3–ICEMS study. *Hyperfine Interact*. Vol. 139–140, pp. 407–416.
12. Hofmann, M., Campbell, S. J. & Kaczmarek, W. A. (2002). Mechanochemical treatment of α-Fe_2O_3: A neutron diffraction study. *Appl. Phys*., Vol. A74, pp. 1233–1235.
13. Hofmann, M., Campbell, S. J., Kaczmarek, W. A. (1996). Mechanochemical Transformation of hematite to magnetite: Structural investigation. *Mater. Sci. Forum*, pp. 228-231, pp. 607-614.
14. Wu, E., Campbell, S. J., Kaczmarek, W. A., Hofmann, M., Kennedy, S. J. & Studer, A. J. (1999). Mechanochemical treatment of hematite-neutron diffraction investigation. *Mate. Sci. Forum*, Vol. 312-314, pp. 121-126.
15. Cornell, R. M. & Schwertmann, U. (2003). *The iron oxides: structure, properties, reactions, occurrences and uses*. Wiley-VCH Verlag GmbH & Co. KGaA, Weinheim,.
16. Heegn, H., Birkeneder, F. & Kamptner, A. (2003). Mechanical activation of precursors for nanocrystalline materials. *Cryst. Res. Technol*., Vol. 38, pp. 7–20.
17. Pourghahramani, P. & Forssberg, E. (2006). Comparative study of microstructural characteristics and stored energy of mechanically activated hematite in different grinding environments. *Int. J. Miner. Process*., Vol. 79, pp. 120–139.
18. Pourghahramani, P. & Forssberg, E. (2006). Microstructure characterization of mechanically activated hematite using XRD line broadening. *Int. J. Miner. Process*., Vol. 79, pp. 106–119.
19. Dieter, G. E. (2001). *Mechanical metallurgy*. 3rd ed., McGraw-Hill.
20. Tromans, D. & Meech, J. A. (2001). Enhanced dissolution of minerals: stored energy, amorphism and mechanical activation. *Miner. Eng*., Vol. 14, pp. 1359–1377.
21. Moshksar, M. M. & Zebarjad, S. M. (1999). Morphology and size distribution of aluminum powder during milling processing. *Iranian Journal of Science & Technology, Transaction B, Engineering*, Vol. 23, No. 3, pp. 239-250.
22. Cottrell, A. H. (1958). *Dislocations and plastic flow in crystals*. pp. 37–41, Oxford University.
23. Kaye, G. W. C. & Labay, T. H. (1986). *Tables of physical and chemical constants*, 5th ed., Longman, London, p. 189.
24. Austin, R. A., McDowell, D. L. & Benson, D. J. (2006). Numerical simulation of shock wave propagation in spatially-resolved particle systems. Modelling simul. *Mater. Sci. Eng.,* Vol. 14, pp. 537–561.
25. Williamson, G. K. & Smallman, R. E. (1956). Dislocation densities in some annealed and cold worked metals from measurements on the x-ray debye–scherrer spectrum. *Philos. Mag*., Vol. 1, pp. 34–35.

26. Williamson, G. K. & Hall, W. H. (1953). X-ray line broadening from filed aluminum and wolfram. *Acta. Metall*., Vol. 1, pp. 22–31.
27. Ohlberg, S. M. & Strickler, D. W. (1962). Determination of percent crystallinity of partly devitrified glass by x-ray diffraction. *J. Am. Ceram. Soc.*, Vol. 45, pp. 170–171.
28. Heegn, H. (1987). Model describing the resistance against structural changes and the hardness of crystalline solids. *Cryst Res Technol*., Vol. 22, pp. 1193–1203.
29. Sugawara, T. & Akaogi, M. A. (2004). Calorimetry of liquids in the system Na_2O-Fe_2O_3-SiO_2. *Am. Miner*., Vol. 89, pp. 1586–1596.